CHIMIA **2002**, *56*, No. 10

Chimia 56 (2002) 553–561

ISSN 0009–4293

Prospects and Limitations of Carbon Nanotube Field Emission Electron Sources

Oliver Gröning[a,b*], Richard Clergereaux[a], Lars-Ola Nilsson[a], Pascal Ruffieux[a], Pierangelo Gröning[a], and Louis Schlapbach[b]

Abstract: Today the most mature technology to produce gated micro field electron emitter arrays is the so-called Spindt-type metal micro-tip process. The drawbacks of the Spindt-type process are the expensive production, the critical lifetime in technical vacuum and the high operating voltages. Carbon nanotubes (CNT) can be regarded as the potential second-generation technology to Spindt-type metal micro-tips. The use of CNT as field enhancing structures in field emission electron sources can bring several advantages such as longer lifetime and operation in poor vacuum due to the high chemical inertness as well as low operation voltages and perhaps most important very low cost production techniques. In the present contribution we show that the field electron emission (FE) of CNT thin films can be accurately described by Fowler-Nordheim tunneling and that the field enhancement factor β influences the emission properties most prominently. We have used scanning anode field emission microscopy to investigate the local field emission properties of randomly oriented carbon nanotube deposits. In the technically interesting applied electric field range of 30 V/μm an emission site density larger than 5×10^6 cm^{-2} could be measured. We will discuss however that emitter degradation at high emission currents limits the full exploitation of this high emission site density. The emission degradation becomes apparent for emission currents in the μA range for a single emitter and the field emission I-V characteristics suggests that power dissipation due high contact or intra CNT resistance is the cause of the emitter degradation. Therefore, although the fundamental properties of CNTs are very favorable for the use as field emission tips, these properties alone will not guarantee their success in this area. Our investigations clearly show that a perfect control of the catalytic CNT growth process is needed for successful CNT field emitter technology, at least for high current applications.

Keywords: Carbon nanotubes · Chemical vapor deposition · Electron emission · Emission degradation · Emission site density

1. Introduction

Field electron emission (FE) describes the physical effect of electrons tunneling from the surface of a solid into vacuum under the action of a strong electric field. This phenomenon was first reported by R.W. Wood in 1897 and occurs when fields of the order of 3×10^9 Vm^{-1} = 3000 Vμm^{-1} are present at the surface [1]. Under these conditions the potential step at the surface confining the electrons to the solid, becomes a potential barrier, which is in first approximation triangular in shape. The typical height of this potential barrier (the work function) is about 5 eV for ordinary metals. When the width of this barrier gets smaller than 2 nm the electrons close to the Fermi energy E_F have a non-vanishing probability to tunnel through the barrier and escape into vacuum. The large electric fields required for FE are extremely difficult to generate on flat surfaces, but can be generated by the field enhancing properties of tip like structures.

When a conducting needle-shaped object at a fixed potential is brought into a homogenous electric field, with the electric field parallel to the needle axis, the electric field at the apex of the needle is enhanced by a factor β called the field enhancement factor. For a needle-shaped object (cylindrical body of height h and radius r with a spherical apex) this factor is in first approximation equal to the aspect ratio h/r [2]. A carbon nanotube with a diameter of 20 nm and a length of 4 μm can therefore exhibit a field enhancement of up to 400. Therefore an applied electric field of 7.5 Vμm^{-1} will be amplified by a factor 400 to the required 3000 Vμm^{-1} at the nanotube apex for field electron emission to occur.

Fig. 1 displays schematically the situation at a metal surface under field emission conditions. On the left hand side an energy diagram of the metal–vacuum interface is shown, where the vertical axis denotes the energy relative to the Fermi energy. The electron density of the metal is simply assumed to be the Fermi-Dirac distribution at

*Correspondence: Dr. O. Gröning[a,b]
[a]Universität Fribourg, Physik Departement
Chemin du musée 3
CH–1700 Fribourg
Tel.: +41 26 300 90 68
Fax: +41 26 300 97 47
E-Mail: oliver.groening@gmx.ch
[b]Eidgenössische Materialprüfungs- und Forschungsanstalt (EMPA)
Feuerwerkerstrasse 39
CH–3602 Thun
Tel. +41 33 228 46 26

T = 300 K (dark gray region). The light gray region in the vacuum depicts the shape of the surface potential barrier at an electric field of 2.7 $Vnm^{-1} = 2.7\times10^9$ Vm^{-1} with the image charge potential included. Under these conditions electrons near the Fermi energy can quantum mechanically tunnel through the barrier. On the right hand side the resulting energy distribution of the emitted electrons is given. At room temperature only electrons close to the Fermi energy can be emitted due to the exponentially decreasing tunneling probability with decreasing energy and due to the exponentially decreasing occupation probability with increasing energy.

The development of field emission electron sources has been hampered for half a century by the fact that tip-like field-enhancing structures are needed to create locally the high electric fields for field electron emission to take place. Usually the higher the field enhancement, the smaller the effective emission area of the tip becomes, as the radius of curvature decreases. Although the field emission current density can easily exceed 10000 Acm^{-2}, the total emission current per single tip remains small as the emitting surface, being the apex of the field enhancing tip, is small. The total current per single tip in field emission rarely surmounts 0.1 mA. As a result field emitters are only used where high brightness rather than high currents are required, as in the case of high resolution transmission or scanning electron microscopes.

The key for reaching planar field emitters of high current density approaching 1 Acm^{-2} resides in the integration of a large number of field-enhancing tips on a surface. Depending on the required emission current density, the density of the emitting tips has to be in the range of 10^6–10^8 cm^{-2}. This limits their size to micron or even submicron dimensions. Carbon nanotubes (CNT) have proven to be ideally suited as field enhancing structures for field emission applications due to their exceptionally high aspect ratios with lengths in the micrometer range and diameters ultimately down to one nanometer [3–5]. Furthermore they can be readily produced in large numbers by relatively simple and cost-effective techniques such as chemical vapor deposition (CVD) [6][7].

When it comes down to creating free electrons in vacuum the method most widely employed is thermionic emission which describes the emission of electrons over the surface potential barrier due to high cathode temperatures. The advantage of thermionic electron sources is their simple operation. In the simplest case it is sufficient to heat a tungsten wire to temperatures of the order of 2000 K. However, thermionic sources have some major drawbacks. They are power-controlled electron sources (*via* the temperature) and therefore direct modulation of the electron emission is rather slow. Further, due to the operation at high temperatures the realization of micrometer-sized emitters is not possible because of insufficient heat dissipation and very large temperature gradients. Micro- and nanosized field electron emitters hold the possibility of miniaturizing vacuum electronic devices such as X-ray tubes, pressure gauges or high frequency amplifiers. In this context CNT thin film emitters offer an attractive possibility to produce the key component of a field emission cathode, namely the field emitting tip, in large numbers using inexpensive processes. Various application prototypes using CNT field emitters have been realized so far, where the color CNT flat panel display developed by Samsung could be the most advanced to hit the multi-billion US$ market.

However, currently the performance of planar CNT field emitters is still limited compared to metal micro-tips with regard to emission site density (active emitter per unit area upon parallel addressing), maximum emission current density and emission current stability. In this paper we show that planar CNT thin film emitters exhibit performances that can compete in principle with any of the metal micro-tip arrays, but that emitter degradation strongly hinders the full exploitation of these performances.

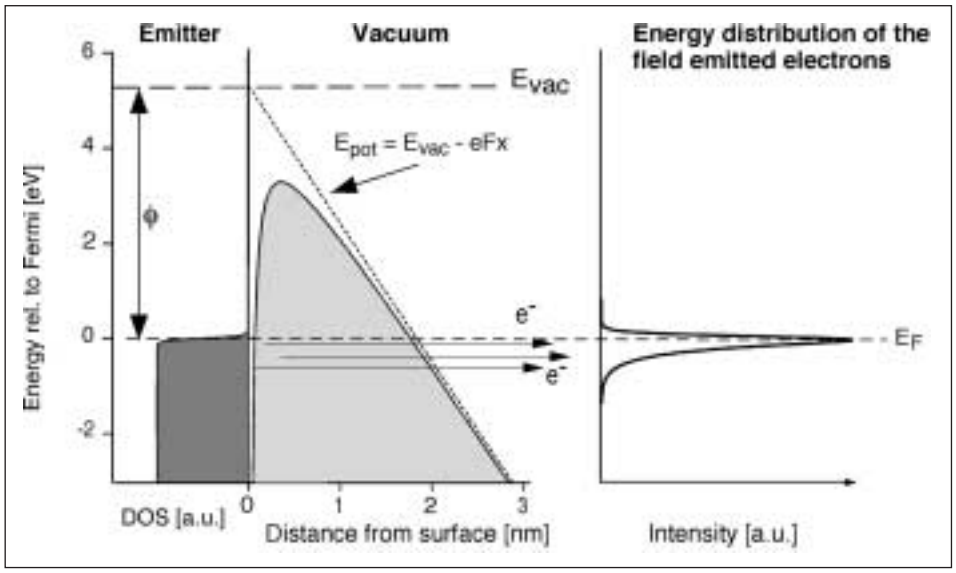

Fig. 1. Schematic illustration of the field electron emission from a metal surface with a work function of 5.3 eV and an electric field F=2.7 Vnm^{-1}. The right hand side diagram shows the resulting emitted total energy electron distribution according to Eqn. (2).

2. Experimental

The carbon nanotube (CNT) thin films used in this study have been grown by chemical vapor deposition (CVD) of a C_2H_2/N_2 gas mixture at substrate temperatures around 750 °C on low resistive p-type Si wafers or by plasma-enhanced CVD of CH_4/H_2 gas mixture at higher temperatures between 800 °C and 1000 °C [8][9]. The growth catalyst was either deposited on the substrate by a thin film (5–10 nm) of sputtered Ni or using a solution of 40 mM $Fe(NO_3)_3$ in ethanol which is sprayed onto the silicon substrate. Using sputtered Ni as catalyst the growth of continuous, randomly oriented CNT films with a mean tube diameter of 30 nm could be achieved, whereas the use of the $Fe(NO_3)_3$–ethanol solution can result in both the growth of continuous or clustered CNT films.

Energy-resolved field emission measurements were carried out in an OMICRON surface analysis system (base pressure: $<10^{-10}$ mbar) equipped with an EA 125 HR electron energy analyzer [10]. The measurements were carried out in the constant analyzer energy (CAE) mode with a pass energy of 5 eV for detailed spectra and 10 eV for series of spectra at different sample biases. With a pass energy of 5 eV and the entrance and exit slits set to minimum, the energy resolution of the analyzer is 35 meV at 100–1000 eV kinetic energy. The high voltage was set to the sample by a Keithley 237 instrument. The ripple on the voltage was always below 5 mV. For the

field emission spectroscopy (FES) measurements the sample could be tilted and rotated to any polar and azimutal angle with respect to the electron analyzer axis. This allowed us to set the sample–detector orientation in such way to obtain maximum count rates. The field emission spectra were measured between 1 pA and 1 nA total emission current, with count rates of 100 to 10^6 cps.

The FE behavior of nanotube thin films was investigated by means of a home-made vacuum scanning anode field emission microscope (SAFEM) operating at a typical base pressure of 10^{-7} mbar [11]. In this set-up the sample is mounted on a computer-controlled piezo-driven x/y-translation stage and a tip of radius 1 μm is approached to the sample in steps of 100 nm, and thereafter held at a constant height d. The tip–sample distance d is chosen larger than the surface roughness of the sample under investigation, typically 5–10 μm. The tip–sample distance can be changed without hysteresis. The FE current I(x,y) at constant applied voltage or the extraction voltage V(x,y) at constant emission current is mapped as a function of the lateral tip position with a Keithley 237 source-measure unit. We call these two measurement modes the constant voltage mode (CVM) and the constant current mode (CCM). In CVM the applied voltage is kept constant (typically 100–300 V) and the measured FE current is recorded as I(x,y). In CCM the extraction voltage V(x,y) applied to the tip is adjusted between 0–1100 V depending on the tip position in order to maintain the FE current at a constant level, *e.g.* 50 nA. Sample areas of several μm up to 800×800 μm^2 were scanned with ~5 μm resolution depending on the tip-sample distance. Tip re-positioning can be achieved with sub-μm accuracy.

3. Results and Discussion

The scanning electron microscopy (SEM) images in Fig. 2 display two typical CVD-grown CNT thin film deposits. Fig. 2a displays a continuous-type CNT film on silicon where sputtered Ni has been used as growth catalyst. Fig. 2b displays a cluster-type CNT film on silicon. For both kinds of CNT structures displayed in Fig. 2 measurable field emission currents can be detected starting from applied electric fields of 1–2 $V\mu m^{-1}$ which correspond to the threshold electric fields often reported for such planar CNT emitters. As we will see later the characterization of the field emission properties using only the value of the threshold field is incomplete and in most cases not even sufficient.

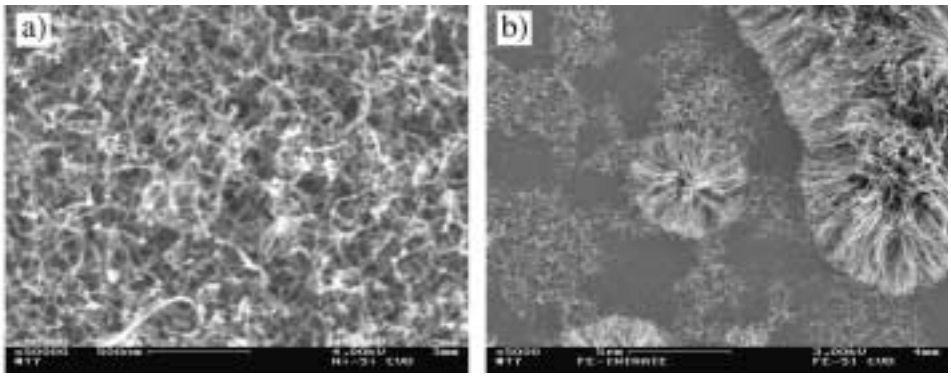

Fig. 2. Scanning electron microscopy images of a) continuous-type multi-walled CNT thin film deposit on p-type Si(100) grown using sputtered Ni as growth catalyst and b) a cluster-type CNT deposit with a $Fe(NO_3)_3$–ethanol solution sprayed on the Si substrate as growth catalyst.

This value of 1–2 $V\mu m^{-1}$ for the applied field has to be compared to the local electric field of 3000 $V\mu m^{-1}$ which is needed according to the Fowler-Nordheim (FN) theory for measurable emission from an ordinary metal surface [12]. Due to the high aspect ratio it seems obvious that local field enhancement is at least partially responsible for the low applied field necessary to observe electron emission from the CNT thin films. It is however not obvious that the electron emission of CNT follows the FN theory, which assumes a free electron gas and a one-dimensional tunneling barrier [13]. According to the FN theory the emission current density j is a function of the electric field E, the emitter work function ϕ according to Eqn. (1)

$$j = \frac{e^3}{4(2\pi)^2\hbar\phi} E^2 \exp\left(-\frac{4\sqrt{2m_e}\phi^{1.5}}{3\hbar eE}\right) \quad (1)$$

In Eqn. (1) the Fowler-Norheim elliptical functions, correcting for the image charge contribution to the tunneling barrier, have been taken to be unity. The total energy distribution P(ε) of the field-emitted electrons near the emitter Fermi energy can be written as:

$$P(\varepsilon) = f(\varepsilon,\varepsilon_F,T)B(E,\phi)\exp\left[C_v\frac{\phi^{0.5}}{E}(\varepsilon-\varepsilon_F)\right] \quad (2)$$

where ε denotes the electron energy, ε_F the Fermi energy of the emitter, ϕ the emitter work function, E the electric field, $f(\varepsilon,\varepsilon_F,T)$ stands for the Fermi-Dirac distribution at temperature T and $B(E,\phi)$ is an energy independent intensity factor. Field emission spectroscopy is ideally suited to check the validity of the Fowler-Nordheim theory for CNT emitters. Fig. 3 shows a series of field emission spectra (FES) measured from a sample of multiwall carbon nanotubes (MWCNT) recorded at room temperature at different applied voltages and therefore different applied fields. The spectrum measured at the highest voltage of 700 V exhibits the highest intensity. The applied voltage was subtracted from the kinetic energy scale of all spectra giving the energy relative to the Fermi energy ε_F. The solid lines are best fits to the data using Eqn. (2). By integrating the spectra over the energy we obtain a value which is proportional to the emission current density. According to the Fowler-Nordheim theory (see Eqn. (1)) the plot of $\ln(j/E^2)$ *vs* 1/E or more general $\ln(I/V^2)$ *vs* 1/V should yield a straight line with negative slope. As can be observed from the inset in Fig. 3 the I-V characteristic of the MWCNT emitter obeys the FN law. The results of the FES investigation on MWCNT therefore show that the FN theory can be used to describe the emission behavior at room temperature with regard to the current–voltage (current–field respectively) characteristic as well as with regard to the energy distribution of the field-emitted electrons. A more detailed analysis of the FES results allows the determination of the emitter work function ϕ, which together with the emitting surface, is the main parameter to describe the current–voltage characteristics of CNT emitter. In the case of MWCNT we can consistently determine a work function ϕ = 4.9±0.3 eV [8][14]. To summarize the results from the FES one can state that the field emission behavior at room temperature of MWCNT is analogous to a metallic tip with 4.9 eV work function. Therefore also in the case of MWCNT emitters the local electric fields present at the nanotube apexes be of the order of 4000 $V\mu m^{-1}$ in order to achieve technologically relevant emission currents in the range of 100 nA per single just as for ordinary metal tips.

Coming back to the threshold fields of the order of 1–2 $V\mu m^{-1}$: this means that the applied electric field is enhanced at the nanotube apex by a factor of about 2000. This

figure however has to be looked at with a great deal of caution as it indicates the highest field enhancement factor of a single CNT on a sample surface where usually many million CNT are present. This shows that the threshold field actually is not a very reliable parameter to quantify the field emission properties of planar CNT field emission cathodes. A more significant characterization of the emission performance of planar CNT cathodes can be achieved by measuring the emission site density (ESD) as a function of the applied field. The ESD is given as the number of emitters per unit area which deliver for a given applied electric field E_A an emission current larger than a given threshold current (*e.g.* 10 nA).

The question, what a technologically relevant and useful emission site density for a nanotube thin film emitter will be, has to be answered in view of the application the emitter is intended for and of course in view of the competing technologies (*e.g.* the Spindt-type metal micro-tip arrays). Comparison with the silicon or metal micro-tip arrays indicates that one should aim at an emission site density of 10^6 to 10^8 cm^{-2} at applied electric fields below 50 $V\mu m^{-1}$. The simplest way of measuring the ESD of a field emission cathode is using a phosphorus-covered screen separated by 50–200 μm from the field emission cathode as anode in a diode type field emission set-up as depicted schematically in the upper panel of Fig. 4. The emitted electrons impinging on the screen created visible light and allow therefore the determination of the emission site density. The lower part of Fig. 4 displays two optical photographs of the electron emission of a CNT cathode using the phosphorus screen set-up for two different applied electric fields. The drawback of this simple method is that it is limited to ESDs below 10^4 cm^{-2}. With higher ESDs the emission sites start to coalesce and the screen becomes completely lit up. However as we have mentioned before the technologically interesting ESD is of the order of 10^6 cm^{-2} or above.

The scanning anode field emission microscope (SAFEM) allows an investigation of the ESD beyond 10^4 cm^{-2} [15]. In the SAFEM the resolution is given by the distance of the scanning anode tip to the cathode surface under investigation. Fig. 5 displays three field enhancement maps β(x,y) of the same region of a randomly oriented MWCNT thin film at different tip sample separations evidencing the increasing resolution with decreasing tip sample distance (Fig. 5a: d = 33 μm; fig. 5b: d = 13 μm; fig. 5c: d = 7 μm). The bright spots in the maps correspond to the emission sites, where the color linearly encodes the local field en-

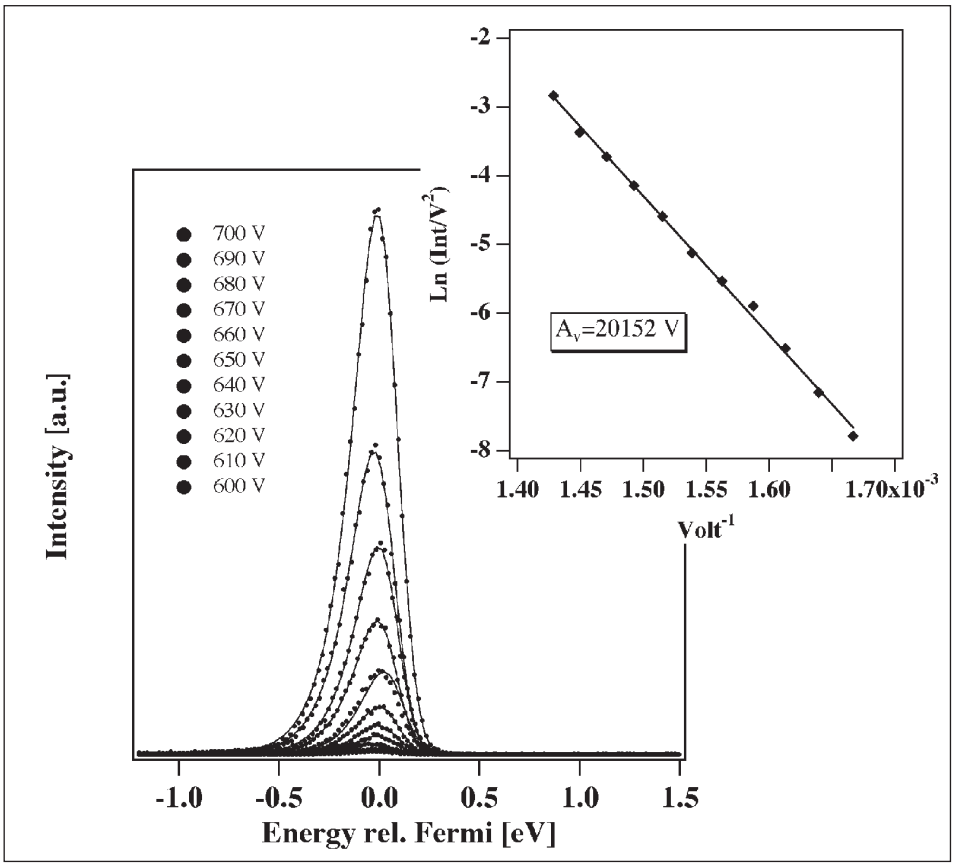

Fig. 3. Series of field emitted total energy distributions from a single MWCNT at different applied voltages and therefore at different electric fields. The spectrum measured at 700 V exhibits the largest intensity. The solid lines are best fits to the experimental data using Eqn. (2). The inset displays the Fowler-Nordheim plot of the integrated spectral intensity yielding a straight line as expected from theory.

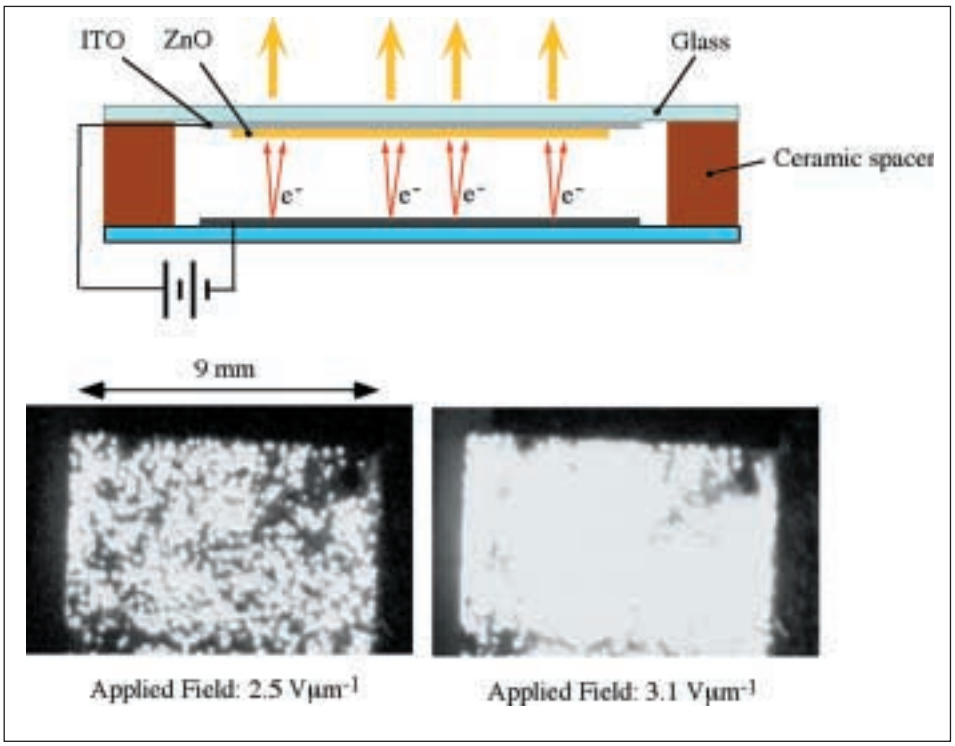

Fig. 4. The upper panel shows the schematic phosphorus screen set-up for the measurement of the emission site density of a planer CNT field emission cathode. The lower panel displays to optical photographs of the emission from a MWCNT cathode on a phosphorus screen for two different applied electric fields.

hancement. The field enhancement maps were generated from voltage maps recorded in the constant current mode (CCV). In this measurement mode the voltage V(x,y) required to obtain a fixed emission current (in this case 11 nA) is recorded as a function of the x-y position of the tip-anode at constant tip–cathode distance. From the FN relation we can deduce that the field at the CNT emitter has to be around 3800 $V\mu m^{-1}$ to emit 11 nA current. Using the following relation we can therefore calculate from the voltage map V(x,y) the field enhancement map β(x,y):

$$\beta(x,y) = \frac{3800[V\mu m^{-1}] \cdot d[\mu m]}{V(x,y)} \quad (3)$$

As can be seen in Fig. 5c the resolution of the SAFEM is given in first approximation as twice the tip sample separation. This means that in order to resolve 10^7 emitter per cm^2 the tip sample separation should be of the order of 2–3 μm. Such a tip sample distance is of the same order of the typical height of the carbon nanotubes and therefore is about the limit of what can be measured without making direct electrical contact between the CNT and the scanning anode.

Fig. 6 displays a high-resolution field enhancement map derived from a SAFEM voltage map recorded at a tip–sample distance of 2–3 μm on a continuous-type, randomly oriented carbon nanotube thin film. The blue diamonds indicate the position of emission sites with a field enhancement factor larger than 130. In the map 164 such emitters could be detected on a sampled surface of 2.4×10^{-5} cm^2 resulting in an emission site density of 6.8×10^6 cm^{-2}. The field enhancement was determined using the assumption, that the local field present at the nanotube apex is 3800 $V\mu m^{-1}$ in order to emit 11 nA, which is the current at which the SAFEM voltage map was recorded. A field enhancement larger 130 therefore means that the applied field is lower than 30 $V\mu m^{-1}$. So that we can conclude, that for MWCNT films as depicted in Fig. 2a an ESD of 5×10^6 cm^{-2} can be achieved at applied electric fields of the order of 30 $V\mu m^{-1}$.

This measurement demonstrates that relatively crude, as-deposited carbon nanotube thin films already exhibit the potential to achieve technologically relevant emission site densities at moderate applied fields. However it is important to point out that the high emission site density indicated above of a few mio. per cm^2 on these samples is to a certain extent academic as it cannot be exploited on large cathode surfaces when the electric field is applied in parallel to the CNT emitter. The reason for this is the large spread in the field enhancement value the individual emitters exhibit for the non-oriented carbon nanotube thin films we discuss here. As can been seen from Fig. 5c the field enhancement factors vary between 300 and 800. This has to be related to the fact that a difference of a factor of two in the field enhancement leads to a difference of 10^3–10^4 in the emission current at the same applied field. It can be shown that the emitters on the randomly oriented CNT cathodes have an exponential frequency distribution of the following type $f(\beta) = C_1\exp(-C_2\beta)$, where β is the field enhancement, C_1 and C_2 are positive constants and $f(\beta)d\beta$ gives the number of emitters per unit surface having a field enhance-

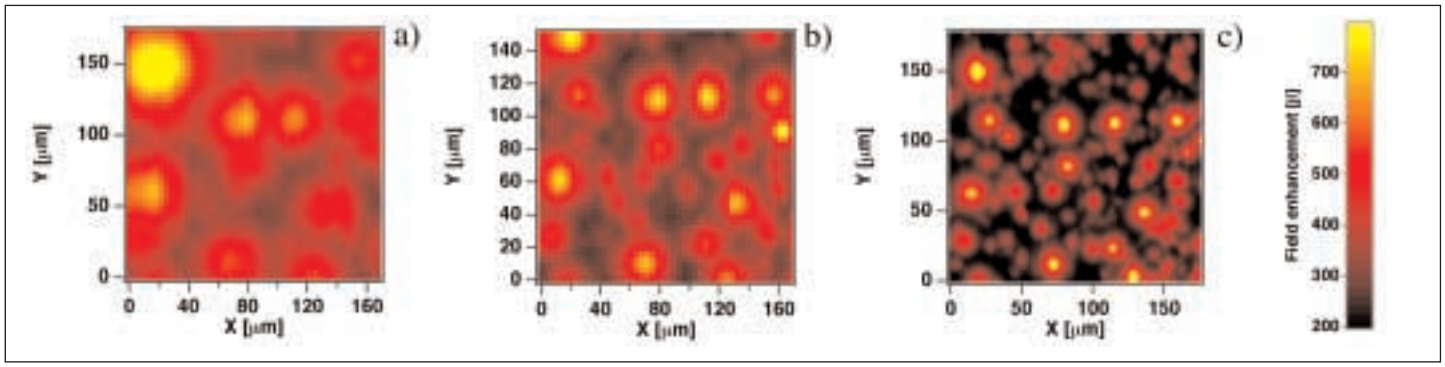

Fig. 5. Scanning anode field enhancement maps β(x,y) of the same region of a continuous type MWCNT cathode as a function of the tip to cathode distance. The tip to cathode distance is d=33 μm in a), d=13 μm in b) and d=7 μm in c) and the constant emission current was 11 nA.

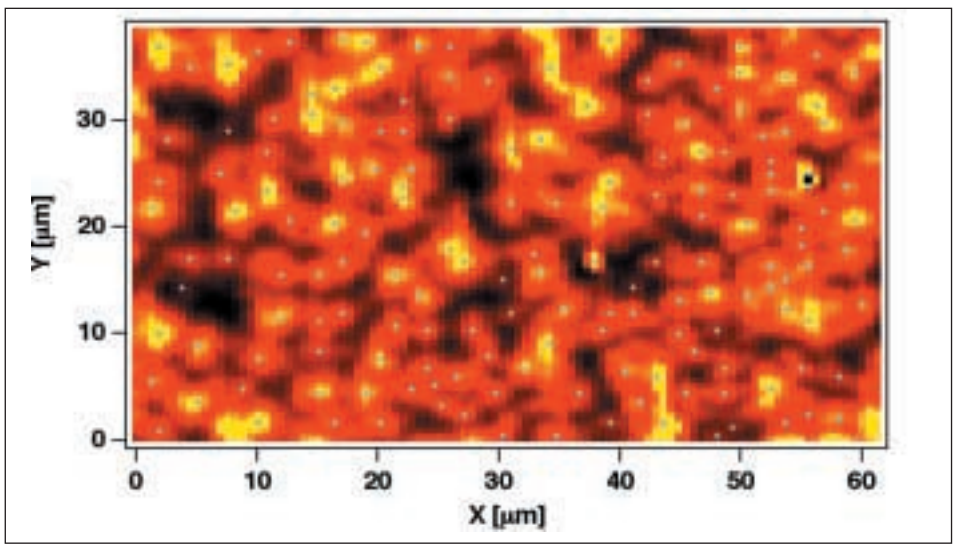

Fig. 6. High-resolution scanning anode field enhancement map β(x,y) on a continuous type MWCNT cathode at a tip to cathode distance of 2–3 μm and at a constant emission current of 11 nA. The blue diamonds indicate the position of emission sites. In total 164 emitters could be identified on a surface area of 2.4×10^{-5} cm^2 giving an emission site density of 6.8×10^6 cm^{-2}. In the map yellow indicates high and black low field enhancement.

ment factor in the interval [β,β+dβ]. This kind of field enhancement distribution results in the situation that on a large cathode surface (*e.g.* 1 cm^2) there are a few very strong emitters of very high field enhancement, typically 1000–2000, which results in the low threshold field of 1–2 $V\mu m^{-1}$. However the emission site density at the threshold field is very low, only 1–10 cm^{-2}. Upon an increase in the applied field the emission site density increases rapidly, but at the same time the emission current from the first few emitters increases exponentially. With a further increase of the applied field the point is reached where the emission current of the first few strong emitters is so large that they are destroyed. From this point on the emission site density hardly increases as a situation is reached where the appearance of new emitters is balanced by the disappearance of old emitters with increasing applied field. For as-deposited MWCNT thin film emitters this point is reached typically at about 10 $V\mu m^{-1}$ with an emission site density of ~10000 cm^{-2} and an emission current density of 1–10 $mAcm^{-2}$. It is clear that under such circumstances the cathode suffers irreversible degradation and that the operation of a cathode under such conditions is highly critical from the point of view of stability and lifetime.

It is crucial to note that emitter degradation at low applied fields is the limiting factor for the performance of carbon nano-tube cathodes. In order to enhance the field emission performance of such cathodes a detailed understanding of the degradation mechanism and subsequently the improvement of the degradation behavior is required.

Fig. 7a displays the voltage map V(x,y) for a constant emission current of 11 nA of a continuous-type, randomly oriented MWCNT cathode with a tip to sample separation of 4–5 μm and Fig. 7b shows the corresponding field enhancement map β(x,y) where the positions of individual emitters are marked by black crosses. Dips in the voltage map as well as peaks in the field enhancement map obviously correspond to individual emitters. Two distinct regions can be identified in the voltage as well as in the field enhancement map. The left hand region characterized by lower field enhancement has been strained by high emission currents above 1 μA per single emitter prior to the displayed measurement, whereas the right hand region has not been subjected to emission currents above 11 nA. Therefore the right hand side shows the genuine emission properties of the MWCNT cathode and the left hand region the emission properties after high current degradation. The degraded region is again subdivided into two regions were the current strain was 1.5 μA and 2.0 μA respectively as indicated by the arrows in the figure. It is obvious from Fig. 7b that in the current strained regions the emitters with high field enhancement are gone and only emitters with lower field enhancement are left. The values at which the current degradation occurs can vary from 500 nA up to a few μA per single emitter. The emitters which are then left over after the degradation with a lower field enhancement are typically very stable and robust, which means that they can sustain emission currents well above 1 μA even up to 100 μA for short periods of time. A closer inspection of the regions strained by 1.5 μA and 2.0 μA shows that the average field enhancement is higher in the region with the lower strain current. This behavior indicates that the high current degradation is linked with the field enhancement, where the critical current for degradation decreases with increasing field enhancement (and therefore increasing aspect ratio). Although there seems to be a link between aspect ratio and degradation a complete understanding of this phenomenon will require effects due to ambient gas composition and pressure, CNT quality, intra-tube and contact resistance as well as adherence of the CNT to the substrate to be included.

Fig. 8 illustrates the degradation of a single emitter as opposed to the collective current degradation behavior displayed in Fig. 7. Fig. 8a and 8b show field enhancement maps (measured at 11 nA emission current) before and after the central emitter (indicated by the blue arrow) has been subjected to high current degradation. The I-V characteristic displayed in Fig. 8c shows that the irreversible degradation occurs abruptly at an applied voltage of 290 V (corresponding to an applied field of 14.5 $V\mu m^{-1}$ and at a current level of 2.2 μA. The degradation manifests itself by a current drop of almost three orders of magnitude. As can be evaluated from the field enhancement maps of Fig. 8a and 8b the value of the field enhancement at this position has decreased from 630 to 250. It has to be pointed out that most probably the emission

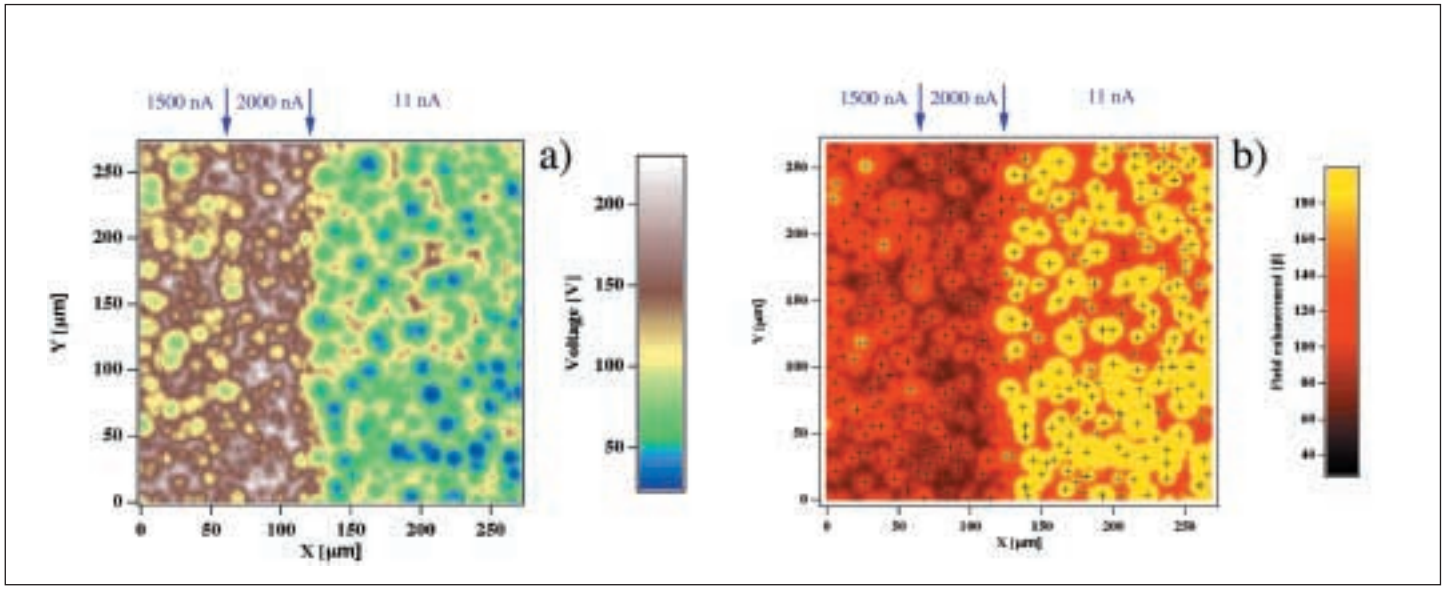

Fig. 7. Scanning anode voltage V(x,y) a) and corresponding field enhancement map β(x,y) b) of a partially high current stressed continuous type MWCNT cathode. The measurements were performed at a tip to cathode distance of 4–5 μm and a constant emission current of 11 nA. Prior to the measurement the regions indicated by the arrows were strained by high emission currents of 1.5 μA and 2.0 μA respectively. The emission degradation in both current strained regions is clearly visible.

after the degradation does not originate from the same nanotube as before but from a tube nearby, which was before concealed by the original emitter.

The black curve in Fig. 8c indicates the theoretical Fowler-Nordheim emission behavior and can be modeled as follows:

$$I = C_1 \cdot V^2 \exp\left[-\frac{C_2}{V}\right] \qquad (4)$$

C_1 and C_2 are positive constants in Eqn. (4) which is equivalent to the Fowler-Nordheim law (1) taking into account the proportionality between the voltage and the field. One can observe that in the low current regime the measured I-V characteristic is well described by the FN law. However above an emission current of about 100 nA a pronounced deviation from the FN behavior can be observed. This kind of current saturation continues to a voltage of about 290 V and an emission current of 2.2 μA, where a sudden and irreversible decrease of the emission current to a value of 7 nA occurs. The emission behavior in non Fowler-Nordheim regime can be modeled using a resistor limitation approach, where it is assumed that there is a voltage drop between the emission site (being the CNT apex) and the electron reservoir (being the electric contact of the CNT). This results in the situation that not the full applied voltage generates the extraction field for the electron emission, but that this voltage is reduced by the product of the emission current and the resistance in the current path, corresponding to the voltage drop in the resistor. Assuming an ohmic resistor the high voltage behavior in Fig. 8c can be modeled reasonably well (see green curve) according to the following relation:

$$I = C_1 \cdot (V - \Delta V)^2 \exp\left[-\frac{C_2}{V - \Delta V}\right] =$$

$$C_1 \cdot (V - R \cdot I)^2 \exp\left[-\frac{C_2}{V - R \cdot I}\right] \qquad (5)$$

Here R denotes the limiting resistor and C_1 and C_2 are the same positive constants as for Eqn. (4). Relation (5) is of course recursive and has to be evaluated numerically. From the emission current and the voltage drop one can estimate the amount of power dissipated in the resistor. In principle the voltage drop could be determined from the model, it has to be stressed however that in order to do so the influence of the voltage drop on the local field should be known. This in turn requires information on the exact location of the voltage drop in the current path and the amount of electrostatic shielding the emitter experiences. Both are generally unknown. The schematic drawings in Fig. 8d and 8e illustrate the possible origins of the voltage drop due to either a high internal resistance in the CNT, *e.g.* due to defects, or a high contact resistance. It can be estimated that the voltage drop in the saturation regime has to be of the order of 10 V which gives, with an emission current of 2 μA, a power of 20 μW dissipated. Taking into account the small volume of the contact of 5×10^{-17} cm^3, which is of the order of the nanotube diameter to the power of three: one estimates a power density in the range of one terra Watt/cm^3 dissipated in the contact. This can easily explain the emission degradation and the observed local substrate melting due to high emission currents.

From this consideration it becomes obvious that operating the emitter in the current saturation regime is always risky as the current saturation is a sign of power dissipation and therefore of possible degradation. From the I-V curve in Fig. 8c it becomes apparent that the voltage window where the emitter can be operated usefully with an emission current between 10 nA and 2 μA is rather small. In the present case this is between 150 V and 300 V although at 300 V degradation has to be expected. This finding can be related generally to MWCNT emitters by realizing that the window of operation for an emitter corresponds to about twice the threshold field. Together with large spread in the field enhancement factor this leads to the limitation in the emission performance of randomly oriented MWCNT thin film emitters. As discussed above the threshold field for macroscopic cathodes of 1 cm^2 is about 2 Vμm^{-1}, the SAFEM investigation however shows that an interesting emission site density of

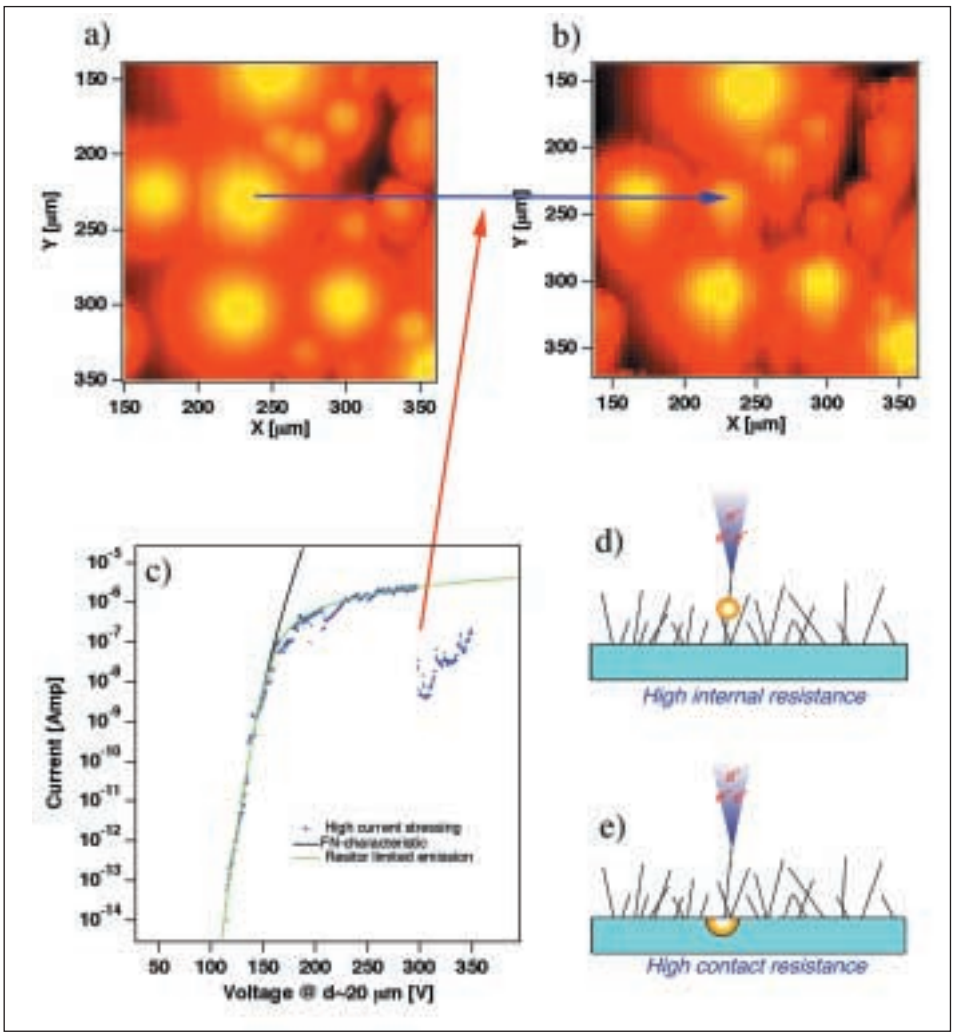

Fig. 8. Single emitter high current degradation measured on a cluster type MWCNT cathode. The field enhancement maps a) and b) show the reduction in the field enhancement factor for the emitter indicated by the blue arrow before a) and after b) the degradation event. In the maps yellow corresponds to high and black corresponds to low field enhancement. Diagram c) displays the I-V characteristic of the degradation where the blue crosses indicate the experimental data, the black solid line the theoretical Fowler-Nordheim behavior and the green solid line the resistor limited I-V behavior. The schematic drawings d) and e) represent emitter degradation due to large power dissipation due to either a high intra tube resistance or due to a high contact resistance.

the order of 10^6 cm^2 is reached only for applied fields above about 25–30 Vμm^{-1}. According to the consideration above we have to expect emitter degradation for fields above about 4–6 Vμm^{-1}. It is therefore not possible to reach the required applied field for the high ESD without very severe emitter degradation.

4. Conclusions

The attractiveness of CNTs for use as field emitters resides in the fact that with a length of a few μm and diameters of down to a few nm they exhibit a large field enhancement β. Furthermore they can be produced in large quantities (with respect for use as field emitters) using relatively simple and inexpensive processes. We have shown using FES that the emission of MWCNTs at room temperature can be regarded as being analogous to the emission from a metallic needle with a work function of 4.9 eV. SAFEM has evidenced that technologically interesting emission site densities above 5×10^6 cm^{-2} can be obtained on continuous-type randomly oriented MWCNT thin film emitters on silicon for applied electric fields of the order of 30 Vμm^{-1}. This performance however cannot be directly exploited due the limitations in the maximum applied field before irreversible emitter degradation occurs. The maximum applied field before degradation occurs can be estimated to be about twice the threshold field. An optimization of the field emission performance of CNT cathodes will require a detailed understanding of the mechanisms involved in emitter degradation. In this complex behavior the contact resistance to the emitting tube will be one important component. Furthermore the spread of the field enhancement factor needs to be controlled in such a way that the desired emission site density can be obtained within an applied electric field corresponding to about twice the threshold field.

Fig. 9 illustrates the effect of electrostatic shielding in nanotube films with different tube density leading to a large spread in field enhancement factors. A quantitative analysis of the computer simulation showed that optimum field emission properties for a nanotube film can be expected, if the mean distance between the tubes is about twice their height. Furthermore it can be seen from Fig. 9 that the field enhancement factor of the tubes in a film shows a wide distribution, as it is influenced by the orientation of the tube with respect to the applied electric field and by the degree of electrostatic shielding a tube receives from its neighboring tubes. In a real nanotube film the differences of length and diameter of the individual tubes will further contribute to the distribution of the field enhancement factor among the nanotubes. This distribution gives rise to inhomogeneous field emission properties.

The simulation shown in Fig. 10a explains why a homogenous emitting CNT film needs an ordered CNT growth. The ideal case of such a CNT growth is displayed in Fig. 10a, where all the tubes have the same height, diameter, orientation and the same spacing from each other. Recent publications have shown well-oriented CNT growth [16–18]. The problem of all these films for FE is that the spacing between the individual CNT is not large enough to prevent electrostatic shielding. It is a big challenge for the nanotechnology to develop the processes required for the deposition of CNT films optimal for FE which need to be efficient and economical at the same time. We are currently seeking in a TOP NANO 21 project of the Swiss Committee for Technology and Innovation (CTI) methods for controlled CNT growth. Fig. 10b displays the SEM image of ordered carbon nanofibers grown using plasma enhanced CVD in collaboration with the University of Cambridge [19].

In the case of flat panel display a CNT-based field emission technology will ultimately need to fulfill the following requirements to be competitive with the current metal tip technology:

I. Growth of individual CNTs at well-defined positions with a tolerance ~100 nm.
II. Growth of individual CNTs with well-defined orientation.
III. Growth of individual CNTs with a well-defined aspect ratio (β = h/r), tolerance dβ/β ~5%.
IV. Massively parallel processes (10^8 tubes per cm^2).
V. Large area deposition (~m^2).
VI. Low cost processes.

Acknowledgement
We would like to acknowledge the financial support of the CTI *via* the TOP NANO 21 project Nr. 5465.1 as well as Ken Teo and William Milne of the engineering department of the University of Cambridge for the growth of ordered arrays of carbon nanofibers.
Received: July 25, 2002

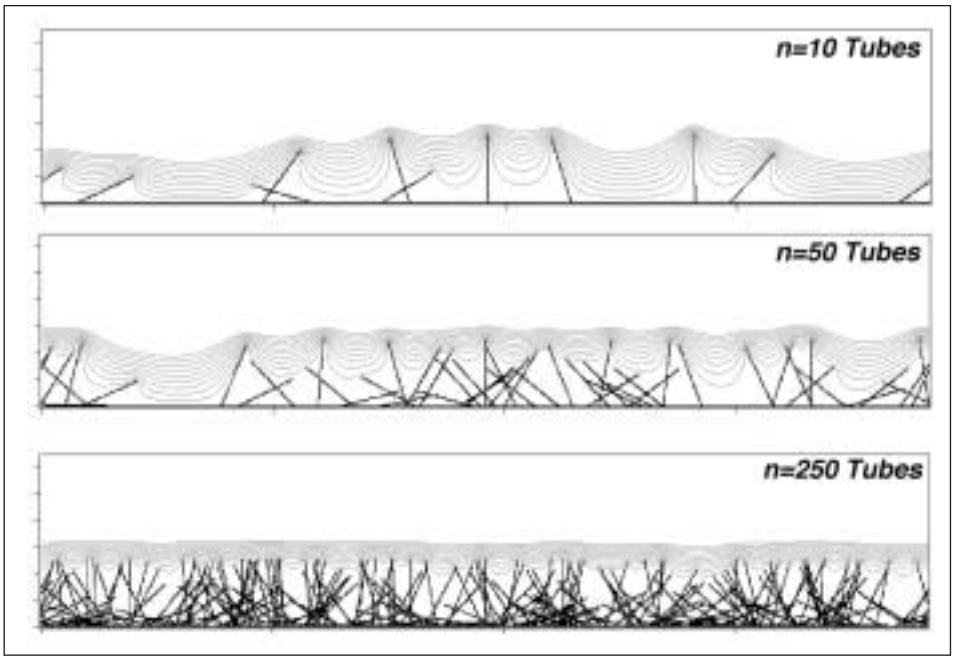

Fig. 9. Simulation of the electric field distribution (indicated by the equipotential lines) on a planar CNT cathode as a function of the CNT density in indicating the effect of increasing electrostatic shielding with increasing tube density.

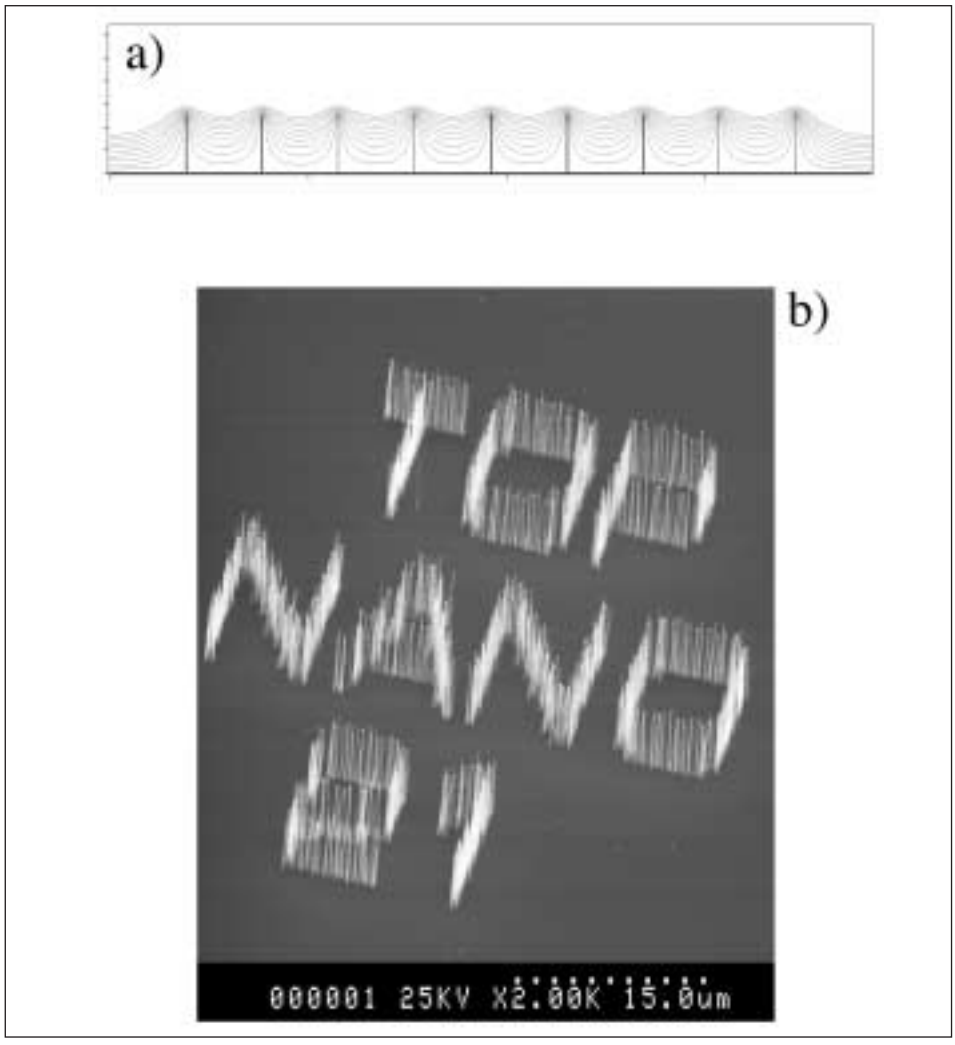

Fig. 10. Panel a) displays the simulation of the electric field distribution (indicated by the equipotential lines) of an ordered arrangement of CNT. Panel b) displays the SEM image of deterministically grown carbon nanofibers using a plasma enhanced CVD process showing the name of the Swiss CTI program Top Nano 21.

[1] J.W. Gadzuk, *Rev. Mod. Phys.* **1973**, *45*, 487.
[2] F. Rohrbach, CERN Report, 71-5/TC-L, 1971.
[3] S. Iijima, *Nature*, **1991**, *354*, 56.
[4] W.A. de Heer, A. Châtelain, D. Ugarte, *Science* **1995**, *270*, 1179.
[5] A.G. Rinzler, J.H. Hafner, P. Nicolaev, L. Lou, S.G. Kim, D. Tomanek. P. Nordlander, D.T. Colbert, R.E. Smalley, *Science* **1995**, *269*, 1179.
[6] S. Iijima, T.W. Ebbesen, P.M. Ajayan, *Nature* **1992**, *358*, 220.
[7] M. Endo, K. Takeuchi, S. Igarashi, K. Kobori, M. Shiraishi, H.W. Kroto, *J. Phys. Chem. Solids* **1993**, *54*, 1841.
[8] O. Gröning, O.M. Küttel, C. Emmenegger, P. Gröning, L. Schlapbach, *J. Vac. Sci. Technol. B* **2000**, *18(2)*, 665.
[9] H. Kind, J-M. Bonard, C. Emmenegger, L-O. Nilsson, K. Hernadi, E. Maillard-Schaller, L. Schlapbach, L. Forro, K. Kern, *Adv. Mater.* **1999**, *11*, 1285.
[10] P. Ruffieux, P. Schwaller, O. Gröning, L. Schlapbach, P. Gröning, Q.C. Herd, D. Funnemann, J. Westermann, *Rev. Sci. Instr.* **2000**, *71*, 3624.
[11] L. Nilsson, O. Gröning, O.M. Kuettel, P. Gröning, L. Schlapbach, *J. Vac. Sci. Technol.* **2002**, *B20*, 326.
[12] I. Brodie, C.A. Spindt, *Advances in Electronics and Electron. Physics* **1992**, *83*, 6.
[13] R.H. Fowler, L.W. Nordheim, *Proc. R. Soc. London, Ser. A.* **1928,** *119*, 173.
[14] O. Gröning in 'Field Emission Properties of Carbon Thin Films and Carbon Nanotubes', PhD Thesis No. 1258, **1999,** Department of Physics, University of Fribourg, Switzerland.
[15] L. Nilsson, O. Groening, C. Emmenegger, O.M. Kuettel, E. Schaller, L. Schlapbach, *Appl. Phys. Lett.* **2000**, *76*, 2071.
[16] S.H. Tsai, C.W. Chao, C.L. Lee, H.C. Shih, *Appl. Phys. Lett.* **1999**, *74*, 3462.
[17] J. Li, C. Papadopoulos, J.M. Xu, M. Moskovits, *Appl. Phys. Lett.* **1999,** *75*, 367.
[18] C. Bower, *Appl. Phys. Lett.* **2000**, *77*, 830.
[19] K.B.K Teo, M. Chhowalla, G.A.J. Amaratunga, W.I. Milne, D.G. Hasko, G. Pirio, P. Legagneux, F. Wyczisk, D. Pribat, *Appl. Phys. Lett.* **2001**, *79*, 1534.